Hindawi Publishing Corporation
International Journal of Corrosion
Volume 2015, Article ID 410120, 15 pages
http://dx.doi.org/10.1155/2015/410120

Research Article

Effect of Piperidin-4-ones on the Corrosion Inhibition of Mild Steel in 1 N H_2SO_4

Glory Tharial Xavier,[1] Brindha Thirumalairaj,[2] and Mallika Jaganathan[2]

[1]*Department of Science and Humanities, Sri Krishna College of Engineering and Technology, Coimbatore, Tamil Nadu 641008, India*
[2]*Department of Chemistry, PSG College of Arts and Science, Coimbatore, Tamil Nadu 641014, India*

Correspondence should be addressed to Mallika Jaganathan; jmpsgcas@gmail.com

Received 20 July 2014; Revised 24 December 2014; Accepted 28 December 2014

Academic Editor: Michael I. Ojovan

The corrosion inhibition of mild steel in 1 N sulphuric acid solution by 2,6-diphenylpiperidin-4-ones with various substituents at 3- and 3,5-positions (01–06) has been tested by weight loss, potentiodynamic polarization, electrochemical impedance spectroscopic methods, and FTIR and UV absorption spectra. The surface morphology of the mild steel specimen has been analyzed by SEM. The effect of temperature (300 to 323 ± 1 K) on the corrosion behavior of mild steel in the presence of the inhibitors (01–06) was studied using weight loss techniques. The effect of anions (Cl^-, Br^-, and I^-) on the corrosion behavior of mild steel in the presence of the same inhibitors was also studied by weight loss method and the synergism parameters were calculated. The adsorption characteristics of the inhibitors have been determined from the results.

1. Introduction

Corrosion inhibitors find vast application in the industrial field as components in acid descaling, oil well acidizing, acid pickling, acid cleaning, and so forth. Most of the effective inhibitors used contain heteroatom such as O, N, S, and multiple bonds in their molecules through which they are adsorbed on the metal surface. It has been observed that adsorption depends mainly on certain physiochemical properties of the inhibitor group, such as functional groups, electron density at the donor atom, π-orbital character, and the electronic structure of the molecule [1–8]. Several researchers investigated the corrosion inhibiting properties of organic compounds on mild steel in acidic medium [9–12]. The aim of this work was to investigate the effect of substitution at 3- and 3,5-positions of 2,6-diphenylpiperidin-4-one on the corrosion inhibition of mild steel 1 N H_2SO_4 solution. Corrosion inhibition was investigated using weight loss, electrochemical impedance spectroscopy (EIS), and potentiodynamic polarization (Tafel) methods and their results were compared.

2. Experimental Details

The variously substituted 2,6-diphenylpiperidin-4-ones (01–06) were prepared via following reported procedures [13, 14]. Mild steel specimens of the following composition have been used all over the present investigations (Carbon: 0.07%, Sulphur: nil, Phosphorous: 0.008%, Manganese: 0.34%, remaining ferrous).

2.1. Methods. In the gravimetric experiment, mild steel specimen of the dimensions 2.5 cm × 1 cm × 0.1 cm has been used. It was polished using 1/0, 2/0, 3/0, and 4/0 emery papers, washed with double distilled water, dried, and finally degreased with the acetone. In this method previously weighed coupon was completely immersed in 100 mL 1 N sulphuric acid with and without inhibitor in an open beaker. After an hour, the corrosion product was removed by washing each coupon using double distilled water. The washed coupons were rinsed with acetone and dried in the air before reweighing. From the average weight loss (mean of three replicates analysis) results, the inhibition efficiency (IE%) of

the inhibitor and the corrosion rate of mild steel (CR) were calculated using the following equations:

$$\text{Corrosion rate } (\text{mmpy}) = \frac{(87.6 \times W)}{(D \times A \times T)}, \quad (1)$$

where W is weight loss in mg, D is density in mg, A is area of exposure in cm^2, and T is time in hours.

Inhibition efficiency has been determined by using the following relationship:

$$\text{IE } (\%) = W_o - \frac{W_t}{W_o}. \quad (2)$$

W_o is weight loss without inhibitor. W_t is weight loss with inhibitor.

The effects of temperature on the corrosion inhibition performance for the variously substituted piperidin-4-ones (01–06) were studied in the range of (300 to 323 ± 1 K).

All the electrochemical measurements were carried out using a glass cell of 100 mL capacity. A platinum electrode and a saturated calomel electrode (SCE) were used as counter and reference electrodes, respectively. The mild steel specimens were placed in the test solution for 10 minutes before electrochemical measurements.

The electrochemical impedance measurements were carried out over the frequency range of 10 KHz to 0.01 Hz carried with AC signed amplitude of the 10 mV at the corrosion potential. The measurements were automatically controlled by Z_{view} software and the impedance diagrams were given as Nyquist plots. From the plots the electrochemical parameters such as double layer capacitance (C_{dL}) and charge transfer resistance (R_{ct}) were calculated. The potentiodynamic polarization measurements were made for a potential range of −200 mV to +200 mV with respect to open circuit potential, at a scan rate of 1 mV/sec. From the plot of E versus $\log I$, the corrosion potential (E_{corr}), corrosion current (I_{corr}) were obtained. Tafel slopes b_a and b_c were obtained in the absence and presence of inhibitors. From the I_{corr} values the inhibition efficiencies were calculated. The corrosion rates and inhibition efficiency were obtained from the relationships:

$$\text{Corrosion rate } (C_R \text{ mmpy}) = 3.2 \times I_{\text{corr}} \left(\text{mA/cm}^2\right) \times \frac{\text{Equivalent weight}}{\text{Density}}, \quad (3)$$

$$\text{IE\%} = \frac{I_{\text{corr}(0)} - I_{\text{corr}(i)}}{I_{\text{corr}(0)}} \times 100,$$

where $I_{\text{corr}(0)}$ is the corrosion current in the absence of inhibitor and $I_{\text{corr}(i)}$ is the corrosion current in the presence of inhibitor.

The surfaces of the corroded and corrosion inhibited mild steel specimens were examined using scanning electron microscopy (JEOL-JSM-35-CF). A Shimadzu FT-IR 8000 Spectrophotometer in the 4000–400 cm^{-1} region using the KBr disc technique was employed to examine the interaction of inhibitors with the metal surface.

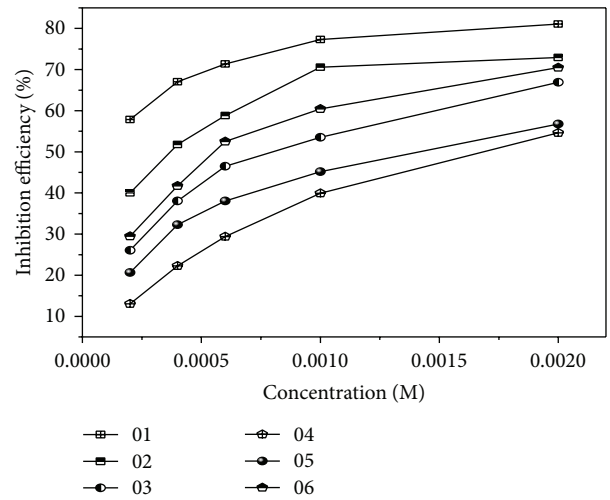

Figure 1: Variation of inhibition efficiency with inhibitor (01–06) concentration for mild steel in 1 N H_2SO_4 at 300 ± 1 K.

3. Results and Discussion

3.1. Effect of Inhibitor Concentration. The corrosion of mild steel in 1 N sulphuric acid solution in the absence and presence of various concentrations (0.2×10^{-3} to 2×10^{-3} M) of inhibitors (01 to 06) was investigated at 300 ± 1 K for 1-hour immersion period using weight loss measurements.

From the weight loss data, plots of inhibition efficiency versus concentration were made and shown in Figure 1. The plots confirm that the inhibition efficiency of all the studied inhibitors (01–06) increases with increase in concentration of the inhibitor.

The extent of inhibition depends on the substituents at 3-position or 3,5-positions of the 2,6-diphenylpiperidin-4-one. At lower concentrations (0.2 to 1×10^{-3} M) the inhibition efficiency increases gradually and it almost reaches saturation above 2×10^{-3} M concentration. The order of inhibition efficiencies of these inhibitors at 300 ± 1 K is 01 > 02 > 06 > 03 > 05 > 04. Analysis of the inhibition efficiencies of inhibitors (01 to 06) reveals that the inhibition efficiency decreases when it is substituted with various groups (methyl, ethyl, isopropyl) at either 3-position of the piperidin-4-one ring or at 3,5-positions of the piperidin-4-one ring. The observed trend can be explained by considering the conformations of substituted piperidin-4-ones and steric hindrance caused by the substitutes.

2,6-Diphenylpiperidin-4-one exists as an equilibrium mixture of both boat and chair conformation [15], whereas 3-alkyl substituted 2,6-diphenylpiperidin-4-one exists in chair conformation with phenyl and alkyl groups at equatorial positions [16–18] (except in compound (06) where one of the C(3)-methyl groups must necessarily be axially oriented). Piperidin-4-ones contain two potential inhibiting groups, namely, the carbonyl group and ring nitrogen [19–22]. The interaction of 2,6-diphenylpiperidin-4-one (01) with the metal surface could occur through either carbonyl group or ring nitrogen. The less electronegativity of nitrogen than oxygen favours ring nitrogen to be the inhibiting site.

Sankarapapavinasam et al. [21] compared the inhibition efficiency of piperidin-4-one and cyclohexanone under identical conditions. They reported that the observed inhibition efficiency of piperidin-4-one (65–80%) was achieved even at very low concentration of the substrate (1.0 mM) while that of cyclohexanone (40%) was achieved at a much higher concentration (100 mM). The inhibition efficiency of unsubstituted piperidine-4-one is higher than that of cyclohexanone. Further the inhibition efficiency of 2,6-diphenylpiperidin-4-one is found to be higher than that of substituted piperidine-4-one. This result reveals that the phenyl rings present in the 2,6-position which are flanking the ring nitrogen play an important role in the inhibition of corrosion. These phenyl groups are in the equatorial position. These equatorial phenyl groups of the substituted piperidin-4-ones lie parallel to the mild steel surface in chair conformation. The interaction between the π electrons of phenyl rings and the mild steel surface prevents the corrosion effectively.

The efficiency of 3-methyl-2,6-diphenylpiperidin-4-one (02) was found to be less than that of 2,6-diphenylpiperidin-4-one (01). This can be explained as follows. In the case of inhibitor (01) the two phenyl rings at 2,6 positions are lying parallel to the metal surface and cause effective interaction with the metal surface, whereas in the case of 3-methyl-2,6-diphenylpiperidin-4-one (02) the methyl group at the C-3 position creates an indirect steric effect known as buttressing effect. It pushes the phenyl rings towards the ring nitrogen thereby changing the orientation of the lone pair of electrons on the nitrogen atom. This effect also decreases the π electron interaction between the phenyl ring and metal surface. By varying the substituents at C-3 position we can study the buttressing effect in detail. Substitution by ethyl, isopropyl, 3,3-dimethyl, and 3,5-dimethyl groups increases the buttressing effect and decreases the inhibition efficiency. In compound (02) methyl, (03) ethyl and in (04) isopropyl group is present. As we move from compound (02) to compound (04), the bulkiness of the group increases, so the buttressing effect increases and, hence, the inhibition efficiency decreases. Generally, the $+I$ effect of alkyl group increases in the order methyl < ethyl < isopropyl. Isopropyl group has greater $+I$ effect than ethyl and methyl and so it is expected to give the highest inhibition efficiency. But in our current investigation inhibitor (04) with isopropyl group shows the least inhibition efficiency, because in this case buttressing effect dominates over $+I$ effect. The inhibition efficiency follows the order 02 > 03 > 04. In addition to this, increase in the degree of chain branching may also lead to lesser protection efficiency owing to higher steric hindrance [23]. Compound (06) with two methyl groups at C-3 position and compound (05) with one methyl group each at 3- and 5-position exhibit lesser inhibition efficiency than compound (02). On correlating experimental results with molecular structures it can be concluded that the increase of steric hindrance at C-3 and C-5 position of substituted piperidin-4-one ring decreased the corrosion inhibiting ability of the studied piperidin-4-ones [24, 25]. One may expect higher inhibition efficiency for inhibitors (06) and (05) when compared to inhibitor (02) because more number of electron releasing methyl groups is present in these inhibitors. On the contrary, inhibitor (02) exhibited higher efficiency. The above observation can be explained as follows. If the number of groups in a molecule increases it leads to overcrowding which causes a strain in the molecule, which results in loss of planarity of the molecule. Since the planarity is disturbed, the phenyl rings may not have much interaction with the metal surface. That is, it may not be able to come closer with the metal surface to have direct contact, which results in lesser protection efficiency for (06) and (05) than inhibitor (02). Moreover the presence of groups which do not act as adsorption centers may not contribute much for the inhibition efficiency of the compound. In addition to this, increase in the degree of chain branching may also lead to lesser protection efficiency owing to higher steric hindrance [23].

3.2. Effect of Temperature. The effect of temperature on the corrosion inhibition performance of inhibitors (01–06) on mild steel in 1 N H_2SO_4 is investigated by weight loss measurements in the temperature range 300 to 323 ± 1 K in the absence and presence of inhibitors (01–06) at 0.4×10^{-3} M concentration. Table 1 shows the values of corrosion rate, surface coverage, and inhibition efficiency obtained from weight loss measurements at various temperatures (300 to 323 ± 1 K). Data in Table 1 suggest that all inhibitors get adsorbed on the mild steel surface at all temperatures studied and corrosion rate increases with increase in temperature in both uninhibited and inhibited solutions. This can be attributed to the fact that the rate of corrosion reaction increases with increase in temperature. But the rate of corrosion is less in inhibited solutions compared with uninhibited solutions. Decrease in inhibition efficiency with increase in temperature is suggestive of physical adsorption mechanism [26, 27] and may be attributed to increase in the solubility of the protective films and of any reaction products precipitated on the surface of mild steel that may otherwise inhibit the corrosion process. As the temperature increases the number of adsorbed molecules decreases, leading to a decrease in the inhibition efficiency. A decrease in inhibition efficiency with the increase in temperature in this case may also be due to weakening of physical adsorption [28].

In order to calculate the activation energy (E_a) for the corrosion process, Arrhenius equation is used

$$C_R = A \exp\left(-\frac{E_a}{RT}\right), \tag{4}$$

where C_R is the corrosion rate, A is the Arrhenius preexponential factor, E_a is the activation energy for the corrosion process, R is the universal gas constant, and T is the absolute temperature.

The apparent activation energies (E_a) at optimum concentration 0.4×10^{-3} M of the inhibitors (01–06) were determined by linear regression between $\log C_R$ and $1/T$ and are represented in Figure 2. Plots of $\log C_R$ versus $1/T$ gave straight line with slope ($-E_a/2.303R$) and intercept A. The linear regression coefficients were close to unity for all the inhibitors analysed. The calculated value of activation energies (E_a) and preexponential factors (A) for the inhibitors are presented in Table 2. Arrhenius law predicts that corrosion

Table 1: Corrosion parameters for mild steel in 1 N H_2SO_4 in the absence and presence of optimum concentration of variously substituted piperidin-4-ones (0.4×10^{-3} M) obtained from weight loss measurements at different temperatures.

Temperature (±1 K)	Inhibitor	Inhibitor efficiency (%)	Corrosion rate (mmpy)	Surface coverage (θ)
300	Blank	—	57.88	—
	(01)	51.76	18.25	0.5038
	(02)	84.62	08.90	0.8462
	(03)	79.62	11.80	0.7962
	(04)	47.31	30.50	0.4731
	(05)	51.15	28.27	0.5115
	(06)	80.16	09.25	0.8016
313	Blank	—	97.06	—
	(01)	33.49	64.56	0.3349
	(02)	57.57	41.18	0.5757
	(03)	49.54	48.98	0.4954
	(04)	28.21	69.68	0.2821
	(05)	30.05	67.90	0.3005
	(06)	52.40	44.65	0.5240
318	Blank	—	136.02	—
	(01)	30.93	93.94	0.3093
	(02)	48.28	70.35	0.4828
	(03)	44.52	75.47	0.4452
	(04)	26.19	100.40	0.2619
	(05)	31.59	93.05	0.3159
	(06)	46.73	73.18	0.4673
323	Blank	—	152.05	—
	(01)	19.91	121.77	0.1991
	(02)	33.82	100.62	0.3382
	(03)	26.65	111.53	0.2665
	(04)	14.93	129.34	0.1493
	(05)	20.50	120.88	0.2050
	(06)	30.15	105.84	0.3015

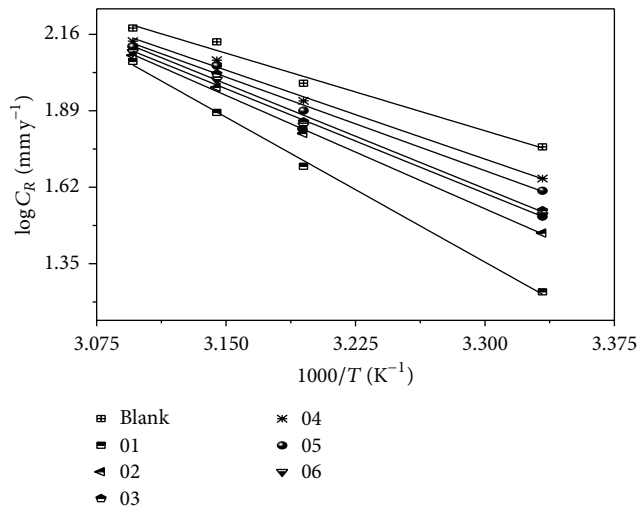

Figure 2: Arrhenius plots of log C_R versus $1/T$ for mild steel in 1 N H_2SO_4 in the absence and presence of inhibitors (01–06) at optimum concentration (0.4×10^{-3} M).

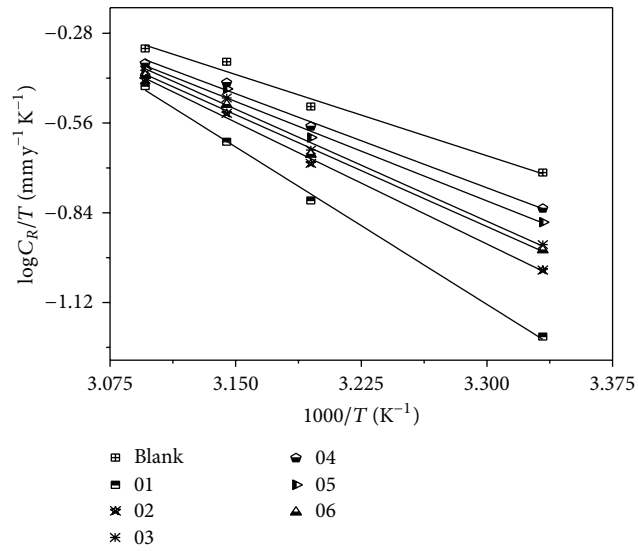

Figure 3: Arrhenius plots of log C_R/T versus $1/T$ for mild steel in 1 N H_2SO_4 in the absence and presence of inhibitors (01–06) at optimum concentration (0.4×10^{-3} M).

rate increases with the temperature and E_a and A may vary with temperature in accordance with (4). Inspection of Table 2 showed that the E_a value for all the inhibitors studied was greater than 20 kJ/mol in both inhibited and uninhibited solutions, which revealed that the entire process is controlled by the surface reaction [29].

The value of E_a for the uninhibited solution was found to be 34.96 kJ/mol and that obtained in the presence of inhibitors (40.07–65.31 kJ/mol) for 01–06. It is clear that activation energy is higher in inhibited solution than in uninhibited solution. The increase in the apparent activation energy in the inhibited solution suggests physical adsorption of the inhibitors on the mild steel surface. The increase in activation energy can also be attributed to an appreciable decrease in the adsorption of the inhibitor on the mild steel surface with increase in temperature. As adsorption decreases more desorption of inhibitor molecules occurs because these two opposite processes are in equilibrium. Due to more desorption of inhibitor molecules at higher temperatures the greater surface area of mild steel comes in contact with aggressive environment resulting in increased corrosion rates with increase in temperature [30]. The very high activation energy in the presence of the inhibitor may be due to the physical adsorption of the inhibitor species on the mild steel surface. This type of inhibitor retards corrosion at ordinary temperatures but inhibition is diminished at elevated temperature [31]. Thus these inhibitors perform well at room temperature.

Figure 3 showed the plot of $\log(C_R/T)$ versus $1/T$ for the corrosion of mild steel in the absence and presence of inhibitors (01–06) in 1 N H_2SO_4. In order to calculate

Table 2: Activation parameters E_a, ΔH°, and ΔS° for the mild steel dissolution in 1 N H_2SO_4 in the absence and presence of variously substituted piperidin-4-ones at optimum concentration (0.4×10^{-3} M).

Inhibitor	Preexponential factor (g cm^{-1} h^{-1})	E_a (kJ mol^{-1})	$E_a - \Delta H^\circ$ (kJ mol^{-1})	ΔH° (kJ mol^{-1})	ΔS° (J mol^{-1})
Blank	6.99×10^7	34.96	2.6	32.38	−45.94
(01)	4.08×10^{12}	65.31	2.6	62.72	45.30
(02)	2.24×10^{10}	52.27	2.6	49.69	05.71
(03)	5.67×10^9	47.22	2.6	44.64	−09.39
(04)	4.22×10^{10}	40.07	2.6	37.49	−30.99
(05)	8.83×10^8	42.17	2.6	39.59	−24.85
(06)	5.28×10^{10}	47.14	2.6	44.56	−09.98

Table 3: Activation parameters K and ΔG°_{ads} for the mild steel dissolution in 1 N H_2SO_4 and in the absence and presence of variously substituted piperidin-4-ones at optimum concentration (0.4×10^{-3} M).

Inhibitors	R^2	Slope	K (mol^{-1})	$-\Delta G^\circ_{ads}$ (kJ mol^{-1})
(01)	1.00	1.17	8075	32.46
(02)	0.99	1.20	3501	30.37
(03)	0.99	1.23	1788	28.70
(04)	1.00	1.17	0756	26.55
(05)	0.99	1.43	1414	28.11
(06)	0.99	1.19	2214	29.23

the activation parameters like ΔH° and ΔS° for the corrosion process, transition state equation [24] was used:

$$C_R = \left(\frac{RT}{Nh}\right) \exp\left(\frac{\Delta S^\circ}{R}\right) \exp\left(-\frac{\Delta H^\circ}{RT}\right), \quad (5)$$

where h is Planck's constant, N is Avogadro's number, R is the universal gas constant, T is the absolute temperature, ΔS° is the entropy of activation, and ΔH° is the enthalpy of activation. Plot of $\log(C_R/T)$ versus $1/T$ gave straight lines with slope $(-\Delta H^\circ/2.303R)$ and intercept $[\log(R/Nh) + (\Delta S^\circ/2.303R)]$, from which ΔH° and ΔS° were calculated and listed in Table 2. Inspection of these data revealed that the entropy of activation for the dissolution reaction of mild steel in 1 N H_2SO_4 in the presence of all inhibitors (0.4×10^{-3} M) is higher (37.49–62.72 kJmol^{-1}) than that in the absence of inhibitors (32.38 kJmol^{-1}). Positive values of enthalpy of activation (ΔH°) in the absence and presence of inhibitor reflect the endothermic nature of the mild steel dissolution process meaning that dissolution of steel is difficult. It is evident from Table 3 that the value of ΔH° increased in the presence of the inhibitor compared to the uninhibited solution indicating higher protection efficiency. This may be attributed to the presence of energy barrier for the reaction; hence the process of adsorption of inhibitor leads to rise in enthalpy of the corrosion process. The values of ΔH° and E_a are nearly the same and are higher in the presence of the inhibitor. This indicates that the energy barrier of the corrosion reaction increased in the presence of the inhibitor without changing the mechanism of dissolution. The value of E_a is found to be larger than the corresponding ΔH° value indicating that the corrosion process must involve a gaseous reaction, simply the hydrogen evolution reaction, associated with a decrease in the total reaction volume [32, 33]. Moreover, the difference value of the $E_a - \Delta H^\circ$ is found to be 2.6 kJ/mol, which is approximately equal to the average value of RT (2.63 kJ/mol). This indicates that the corrosion process is a unimolecular reaction as it is characterized by the following equation:

$$E_a - \Delta H^\circ = RT. \quad (6)$$

This result shows that the inhibitors acted equally on E_a and ΔH°.

On comparing the values of the entropy of activation (ΔS°) in Table 2, it is clear that the positive entropy of activation is obtained in the presence of inhibitors, while negative value (−45.94 Jmol^{-1}) is observed in the case of free 1 N H_2SO_4 solution. Such variation is concerned with the phenomenon of ordering and disordering of the inhibitor molecules at the electrode surface and could be explained as follows. The adsorption of organic inhibitor molecules from the aqueous solution can be regarded as a quasisubstitution process between the organic compounds in the aqueous phase and water molecules at the electrode surface. The adsorption of inhibitors on the mild steel surface is accompanied by desorption of water molecules from the surface. Thus while the adsorption process for the inhibitor is believed to be exothermic and associated with a decrease in entropy of the solute, the opposite is true for the solvent. The thermodynamic values obtained are the algebraic sum of the adsorption of organic molecules and desorption of water molecules. Hence, the gain in entropy is attributed to the increase in solvent entropy and to more positive water desorption enthalpy. The positive values of ΔS° also suggest that an increase in disordering takes place on going from reactants to the metal/solution interface [26], which is the driving force for the adsorption of inhibitors onto the mild steel surface.

3.3. Adsorption Isotherm. Organic molecules are used to inhibit corrosion as they are adsorbed on the metal solution interface. The adsorption depends on the nature of the inhibitor, its conformation in aqueous solution, chemical composition of the medium, nature of the metal surface, temperature, and electrochemical potential at the metal solution interface. Various adsorption isotherms (Henry, Frendlich, Langmuir, Frumkin, and Temkin) have been tried for the inhibitors (01–06) on the mild steel surface in acidic medium at room temperature. The correlation coefficients (R^2) were

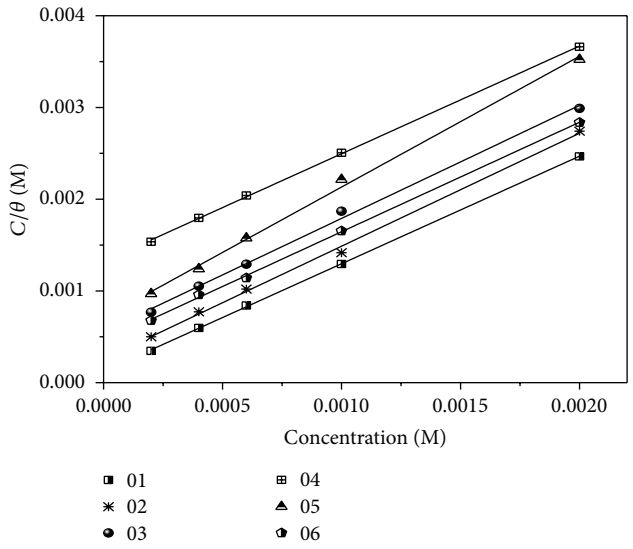

Figure 4: Langmuir isotherm plots for adsorption of inhibitors (01–06) on the mild steel in 1 N H_2SO_4.

used to determine the best fit. For the studied inhibitors best fit was obtained with Langmuir adsorption isotherm.

The Langmuir isotherm is given by the following equation:

$$\frac{C}{\theta} = \frac{1}{K} + C, \tag{7}$$

where K is the equilibrium constant of the adsorption process and C is the molar concentration of inhibitor. The plot of C/θ versus C gave straight line (Figure 4). The linear regression coefficients (R^2) are almost equal to unity. Though the plot of C/θ versus C is linear, the slope obtained is found to deviate from unity. The deviation of the slope from unity might be due to interaction among the adsorbed species on the surface of the mild steel specimen [34–39] or the adsorbate occupies more than one adsorption site on the metal surface. Similar behavior was observed by several researchers [40–43] and has suggested the modified Langmuir adsorption isotherm. Langmuir's adsorption isotherm parameters are presented in Table 3.

The values of equilibrium constant K calculated using Langmuir (8) isotherm are presented in Table 3. A large value of K obtained indicates more efficient adsorption, and hence better inhibition efficiency. The free energy of adsorption (ΔG°_{ads}) is related to the adsorption constant (K) with the following equation:

$$K = \frac{1}{55.5} \exp\left(\frac{-\Delta G^{\circ}_{ads}}{RT}\right), \tag{8}$$

where the value of 55.5 is the concentration of water in solution expressed in molL^{-1}. The ΔG°_{ads} values obtained from Langmuir were calculated at room temperature and are listed in Table 3. The large negative values of ΔG°_{ads} indicate the spontaneity of the adsorption process and the stability of the adsorbed species on the mild steel surface. In general, the values of ΔG°_{ads} of the order of −20 kJ/mol or lower indicate a physisorption [44] while those more negative than −40 kJ/mol involve sharing or transfer of electrons from the inhibitor molecules to the metal surface to form a coordinate type of bond (chemisorption) [45]. It is clear from Table 3 that the calculated ΔG°_{ads} values are in the range between 26.55 and 32.46 kJ/mol for H_2SO_4 solution for optimum concentration (0.4×10^{-3} M) of the inhibitor. This indicates that the adsorption of these inhibitors on the mild steel surface may involve complex interactions involving both physical adsorption and chemical adsorption [46].

It is well-known that surface charge density and zero charge potential of metals play an important role in the process of the electrostatic adsorption [47]. The surface charge of the metal is due to the electric field existing at the metal/solution interface [48]. The surface charge can be defined by the position of E_{corr} with respect to the respective potential of zero charge (PZC) $E_{q=0}$. When the difference $u = (E_{corr} - E_{q=0})$ is negative, the electrode surface acquires a negative net charge and the adsorption of cations is favoured. On the contrary, the adsorption of anions is favored when you become positive. Generally mild steel surface is positively charged in 1 N H_2SO_4 solution [49, 50]. However the inhibitors under investigation, namely, the 2,6-diphenylpiperidin-4-ones, are protonated (piperidinium cation) in acidic solutions and exist in equilibrium with the corresponding molecular form.

The inhibitors studied have ΔG°_{ads} value between 26.55 and 32.46 kJ/mol for 1 N H_2SO. This indicates that the inhibitors adsorb on the mild steel surface through both modes of adsorption (physical adsorption and chemical adsorption) in both acid media. The K values increase in the order of (04) < (05) < (03) < (06) < (02) < (01) which is the same as the order followed by inhibition efficiency obtained from weight loss method.

3.4. Synergistic Effect. It is generally accepted that the presence of halide ions in acidic media synergistically increases the inhibition efficiency of most of the organic compounds. The halide ions are able to improve adsorption of the organic cations by forming intermediate bridges between positively charged metal surface and the positive end of the organic inhibitor [51]. For studying the synergistic inhibitive effect of halide ions, an optimum concentration (0.4×10^{-3} M) of variously substituted 2,6-diphenylpiperidin-4-ones is taken (Scheme 1) and to each of these inhibitors 1×10^{-3} M KCl/KBr/KI is added and the inhibition efficiencies were found using weight loss method and the observations are presented in the Table 4 for 1 N H_2SO_4. Analysis of the results indicates a further reduction in corrosion rate; that is, the inhibition efficiency of the inhibitors was enhanced by the addition of the anions (1×10^{-3} M KCl/KBr/KI).

As far as the inhibition is concerned, it is generally assumed that the adsorption of the inhibitors at the metal/aggressive solution interface is the first step in the inhibition mechanism [52]. The dissolution of mild steel is reduced by either adsorption of the inhibitor molecule on the mild steel surface or blocking the active centers available for corrosion.

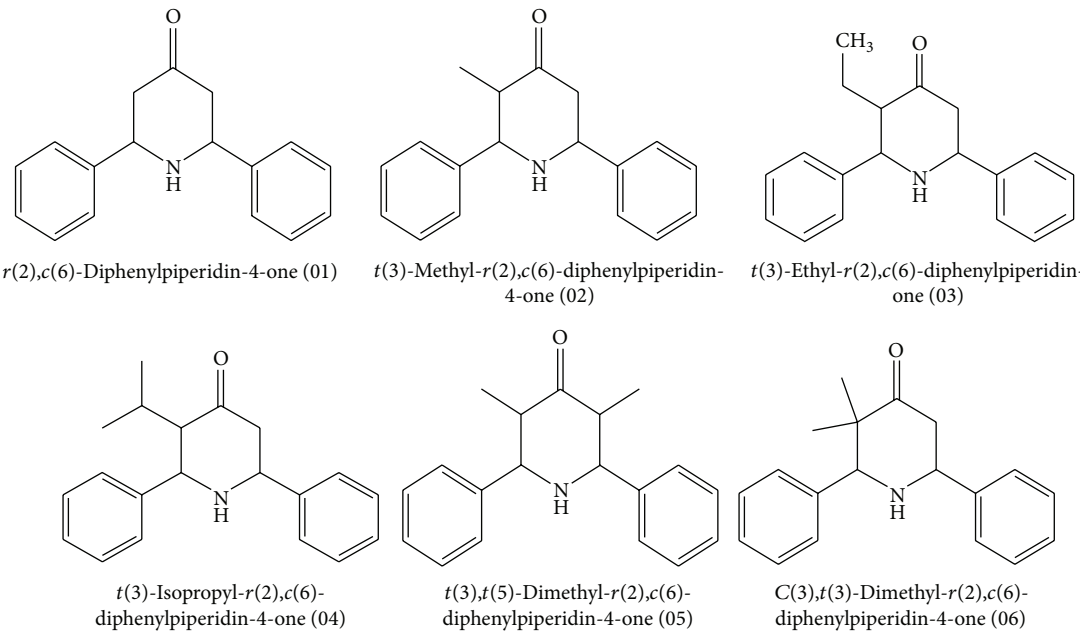

r(2),*c*(6)-Diphenylpiperidin-4-one (01)

t(3)-Methyl-*r*(2),*c*(6)-diphenylpiperidin-4-one (02)

t(3)-Ethyl-*r*(2),*c*(6)-diphenylpiperidin-4-one (03)

t(3)-Isopropyl-*r*(2),*c*(6)-diphenylpiperidin-4-one (04)

t(3),*t*(5)-Dimethyl-*r*(2),*c*(6)-diphenylpiperidin-4-one (05)

C(3),*t*(3)-Dimethyl-*r*(2),*c*(6)-diphenylpiperidin-4-one (06)

Scheme 1: Structures of variously substituted 2,6-diphenylpiperidin-4-ones (01–06).

Table 4: Inhibition efficiency and synergism parameter of variously substituted 2,6-diphenylpiperidin-4-ones (0.4×10^{-3} M) and KCl, KBr, and KI (1×10^{-3} M) systems in 1 N H_2SO_4 solution.

Inhibitors	Without KCl, KBr, and KI IE (%)	KCl		KBr		KI	
		IE (%)	S_θ	IE (%)	S_θ	IE (%)	S_θ
(02)	51.76	61.08	1.14	72.38	1.47	87.44	2.69
(03)	38.03	53.97	1.24	66.10	1.54	82.84	2.53
(04)	22.27	36.40	1.12	50.20	1.31	71.12	1.88
(05)	32.26	45.19	1.14	58.16	1.36	76.99	2.06

It is well-known that the adsorption process is made possible due to the presence of heteroatoms such as N and O which are regarded as active adsorption centers. As discussed earlier, the inhibitors studied (01–06) contain nitrogen, oxygen, and two phenyl rings with π electrons. The compound could be adsorbed by the interaction between the lone pair of electrons of the oxygen and nitrogen atoms or the electron rich π systems of the aromatic rings and the mild steel surface. This process as earlier reported by Umoren and Ebenso [53] may be facilitated by the presence of vacant d-orbital in steel. In addition to the molecular form, piperidin-4-ones can be present as a protonated species in acidic solutions. Generally mild steel surface is positively charged in H_2SO_4 solution, so direct adsorption of a protonated species (piperidinium cation) on the positively charged mild steel surface is difficult. In order to facilitate the adsorption of piperidinium cation on the mild steel surface, halide ions are added to the aggressive medium. The added halide ions being negatively charged are attracted to the positively charged mild steel surface and are adsorbed on metal surface; this leads to development of excess negative charge at metal solution interface, thus lending the mild steel surface negative. Now electrostatic interaction occurs between the positively charged nitrogen atom in the piperidinium cation and negatively charged mild steel surface [54] resulting in physisorption of the inhibitor on the mild steel surface thereby inhibiting the corrosion process. From the above discussion it is clear that the addition of halide ions to the aggressive medium facilitates the adsorption of the piperidin-4-ones on the metal surface.

From Table 4 it is clear that the synergistic ability of the halides increased in the order $Cl^- < Br^- < I^-$ and similar observation has been reported by several researchers [55, 56]. The inhibition efficiency values increase significantly on moving from Cl^- to Br^- to I^-. In other words the surface coverage (θ) value increases in the same order. This is similar to the findings of Oguzie et al., [41]. They have reported that the corrosion inhibitor synergism results from increased surface coverage arising from the ion pair interaction between the organic cation and the anions. The great influence of the iodide ion is often attributed to its large ionic radius, high hydrophobicity, and low electronegativity compared to the other halide ions. In addition, the more stable chemisorption of I^- ions because of the easy deformability of their electron shells also results in higher inhibition effect. This stabilization

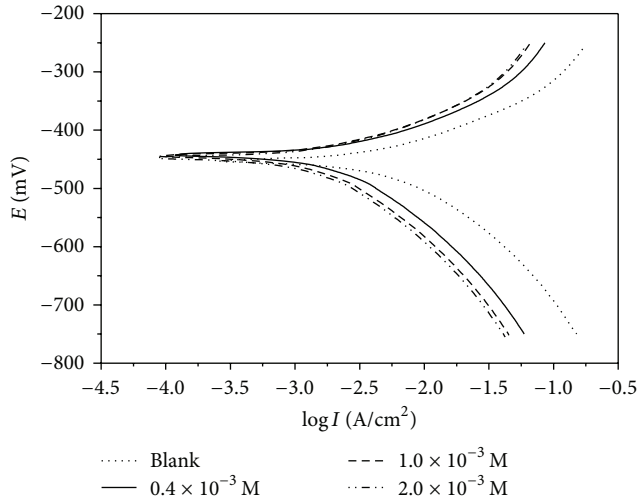

FIGURE 5: Polarization curves for mild steel in 1N H_2SO_4 in the absence and presence of different concentration of inhibitor (01).

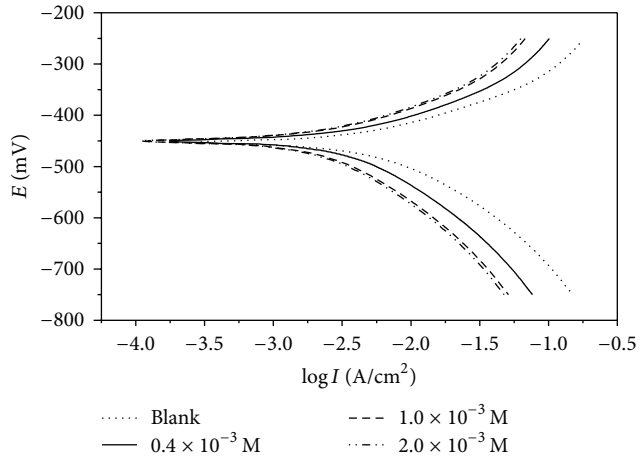

FIGURE 6: Polarization curves for mild steel in 1N H_2SO_4 in the absence and presence of different concentration of inhibitor (02).

may be caused by the interaction between the inhibitor and I^- ions. This interaction enhances the inhibition efficiency to a considerable extent due to the increase of the surface coverage in the presence of iodide ions. According to Hackerman and Makrides [57], the halide ions in general and the iodide ions in particular prevent the steel dissolution in acid solution by a strong interaction with the metal surface, possibly through chemisorption.

The synergism parameter S_θ is evaluated using the relationship given by several authors [58–60]:

$$S_\theta = \frac{1 - \theta_{1+2}}{1 - \theta'_{1+2}}, \tag{9}$$

where θ_1 is surface coverage by the halide ion. θ_2 is surface coverage by the inhibitor, $\theta_{1+2} = (\theta_1 + \theta_2) - (\theta_1\theta_2)$, and θ'_{1+2} is measured surface coverage for the inhibitor in combination with halide ion.

The synergism parameters derived from the inhibition efficiency values obtained from weight loss measurements are summarized in Table 4. It is evident from Table 4 that the S_θ values are greater than unity which indicates that the improved inhibition efficiency caused by the addition of halide ions to the inhibitors is only due to synergistic effect. The highest values of S_θ for I^- ions confirm the highest synergistic influence of I^- ions among halides.

3.5. Potentiodynamic Polarization Measurements. Polarization curves for mild steel in 1N H_2SO_4 solutions at room temperature without and with addition of different concentrations of inhibitors (01–06) are shown in Figures 5–10. The anodic and cathodic current potential curves are extrapolated up to their intersection at the point where corrosion current density (I_{corr}) and corrosion potential (E_{corr}) are obtained. The electrochemical parameters I_{corr}, E_{corr}, anodic,

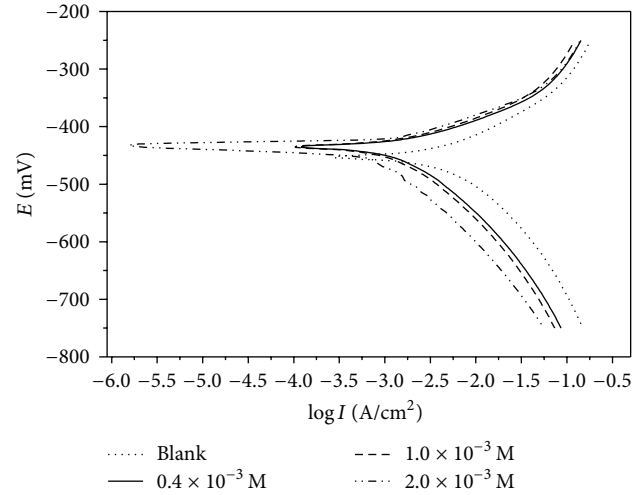

FIGURE 7: Polarization curves for mild steel in 1N H_2SO_4 in absence and presence of different concentrations of inhibitor (03).

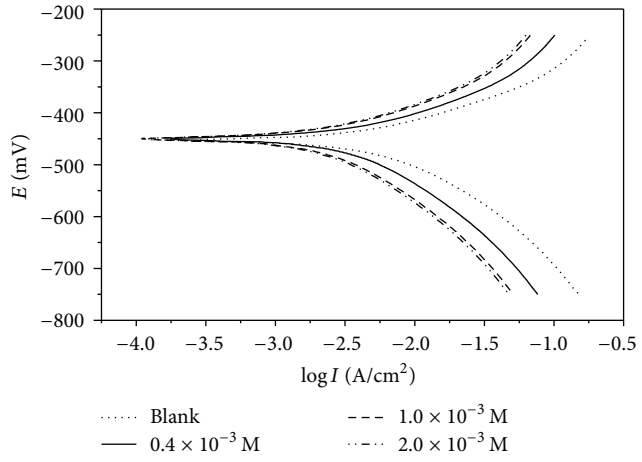

FIGURE 8: Polarization curves for mild steel in 1N H_2SO_4 in the absence and presence of different concentration of inhibitor (04).

Table 5: Polarization parameters for mild steel in 1 N H_2SO_4 in the absence and presence of different concentrations of variously substituted piperidin-4-ones.

Inhibitor	Concentration (10^{-3} M)	$-E_{corr}$ (mV vs SCE)	I_{corr} (mA/cm^2)	b_a (mV/dec)	b_c (mV/dec)	Corrosion rate (mmpy)	Inhibition efficiency (%)
—	Blank	467	12.85	171	250	292.24	Nil
(01)	0.4	454	04.37	133	250	099.25	66.03
	1	462	03.03	133	225	068.82	76.44
	2	456	02.53	116	225	057.51	80.32
(02)	0.4	476	06.25	170	229	142.15	51.35
	1	471	03.83	155	221	087.04	70.21
	2	465	03.55	145	229	080.67	72.39
(03)	0.4	472	08.04	162	266	182.70	37.47
	1	467	06.03	145	250	137.00	53.11
	2	479	04.33	125	225	098.34	66.34
(04)	0.4	445	10.09	154	291	229.47	21.46
	1	476	07.80	180	266	177.31	39.31
	2	477	05.92	145	250	134.50	53.96
(05)	0.4	456	08.71	133	250	198.03	32.22
	1	458	07.05	155	266	160.23	45.16
	2	475	05.70	145	208	129.58	55.65
(06)	0.4	476	07.23	142	250	164.34	43.75
	1	463	05.12	142	250	116.34	60.18
	2	469	03.87	154	238	088.05	69.86

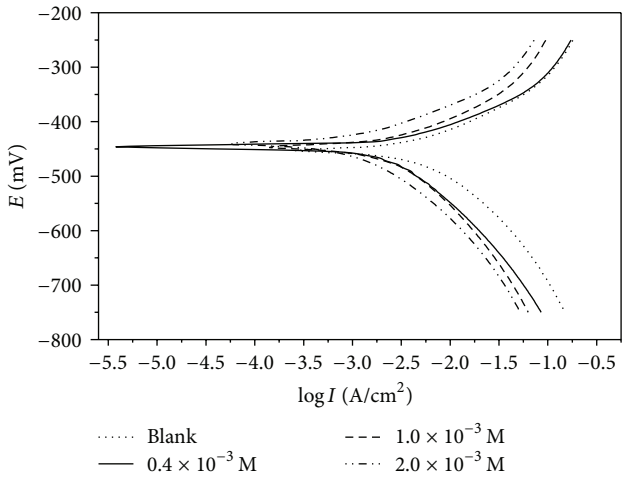

Figure 9: Polarization curves for mild steel in 1 N H_2SO_4 in the absence and presence of different concentration of inhibitor (05).

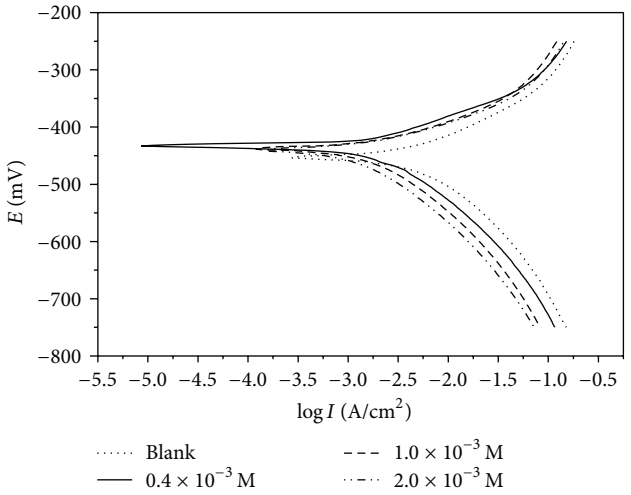

Figure 10: Polarization curves for mild steel in 1 N H_2SO_4 in the absence and presence of different concentration of inhibitor (06).

and cathodic Tafel slopes (b_a and b_c) obtained from polarization measurement are listed in Table 5. The inhibition efficiency was calculated from the expression:

$$\text{IE}\,(\%) = I_{\text{corr}(0)} - I_{\text{corr}(i)} \times \frac{100}{I_{\text{corr}(0)}}, \tag{10}$$

where $I_{\text{corr}(0)}$ and $I_{\text{corr}(i)}$ are corrosion current densities obtained in the absence and presence of inhibitors, respectively. It is clear from Table 5 and Figures 5–10 that the addition of inhibitors to 1 N H_2SO_4 solution brings about a change in both the anodic and cathodic Tafel slopes. These results suggested that the addition of the studied inhibitors reduces the anodic dissolution and also retards the cathodic hydrogen

Table 6: Impedence parameters for mild steel in 1 N H_2SO_4 in the absence and presence of optimum concentration (0.4×10^{-3} M) of variously substituted piperidin-4-ones.

Inhibitors	R_{ct} ($\Omega\,cm^2$)	C_{dl} ($\mu F\,cm^{-2}$)	Inhibition efficiency (%)
Blank	6.548	59.44	Nil
(01)	19.55	22.88	66.51
(02)	13.60	30.39	51.85
(03)	10.60	37.20	38.23
(05)	09.62	42.45	31.93
(06)	11.26	35.89	41.85

evolution reaction, indicating that these inhibitors influence both cathodic and anodic inhibition reactions. Further the addition of inhibitors decreased the corrosion current density (I_{corr}) significantly, which further decreases with increase in concentration of the inhibitors ($0.4–2 \times 10^{-3}$ M) and reaches a minimum value at 2×10^{-3} M concentration of inhibitors. According to Li et al. [61], if the displacement in E_{corr} is >85 mV with respect to E°_{corr} (blank), the inhibitor can be viewed as a cathodic or anodic type. In our study the maximum displacement was found to be (12) mV, which indicates that the inhibitors could be considered as mixed type [62]. The behavior of Tafel slopes b_a and b_c also suggested mixed type of behavior for the inhibitors. Therefore, all the studied inhibitors can be classified as mixed inhibitors for mild steel in 1 N H_2SO_4 solution. The inhibition efficiency was found to increase with increase in concentration of the inhibitors. The values of inhibition efficiency obtained from polarization measurements are almost equal to that obtained from impedance analysis and weight loss measurements. The inhibition efficiency values obtained follow the order

$$(01) > (02) > (06) > (03) > (05) > (04).$$

The above trend is the same as that obtained from weight loss measurement.

3.6. Electrochemical Impedance Measurements. The corrosion behavior of mild steel in acidic solution in the absence and presence of optimum concentration (0.4×10^{-3} M) of inhibitors (01–06) was investigated by the electrochemical impedance spectroscopy method at 300 ± 1 K and the impedance parameters R_{ct} and C_{dl} derived from these investigations are given in Table 6. Nyquist plots of mild steel in inhibiting and uninhibited acidic solutions containing an optimum concentration (0.4×10^{-3} M) of inhibitors are shown in Figure 11. The semicircular nature of impedance diagrams indicates that the corrosion of mild steel is mainly controlled by a charge transfer process, and the presence of the inhibitor does not affect the dissolution mechanism of mild steel [63]. The impedance spectra of the Nyquist plots were investigated by fitting the experimental data to a simple equivalent circuit model as shown in Figure 12, which includes the solution resistance R_s and the double layer capacitance C_{dl} which is placed in parallel to the charge transfer resistance R_{ct}.

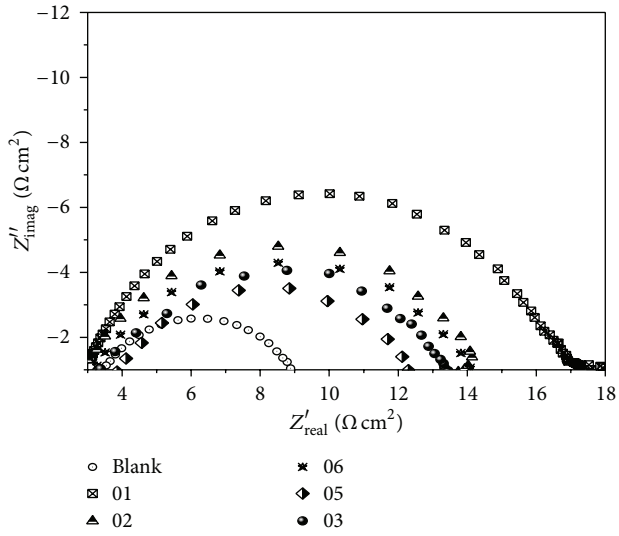

Figure 11: Nyquist plots of mild steel in 1 N H_2SO_4 in the absence and presence of optimum concentration of various inhibitors (01–06).

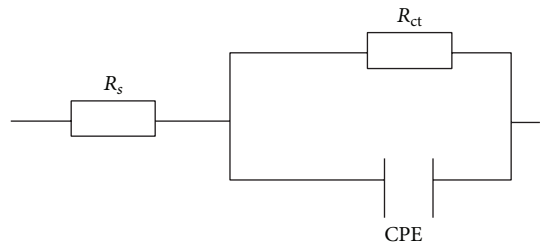

Figure 12: Equivalent circuit model for fitting impedance spectra.

The charge transfer resistance R_{ct} values are calculated from the difference in impedance at low and high frequencies. The R_{ct} value is a measure of electron transfer across the mild steel surface and it is inversely proportional to the corrosion rate. The double layer capacitance C_{dl} was calculated at the frequency f_{max} at which the imaginary component of the impedance is maximal using the equation [64]

$$C_{dl} = \frac{1}{2\pi f_{max} R_{ct}}. \quad (11)$$

Analysis of the data presented in Table 6 indicates that the magnitude of R_{ct} value increased while that of C_{dl} decreased with the addition of inhibitors to 1 N H_2SO_4 medium at optimum concentration of inhibitors. The decrease in C_{dl} values results from the adsorption of the inhibitor molecules at the metal surface. The double layer between the charged metal surface and the solution is considered as an electrical capacitor. The adsorption of inhibitors on the mild steel surface decreases its electrical capacity as they displace the water molecules and other ions originally adsorbed on the surface leading to the formation of a protective adsorption layer on the electrode surface which increases the thickness of the electrical double layer. The thickness of this protective layer

(d) is related to C_{dl} in accordance with Helmholtz model, given by the following equation [27]:

$$C_{dl} = \frac{\varepsilon \varepsilon_o A}{d}, \quad (12)$$

where ε is the dielectric constant of the medium and ε_o is the permittivity of free space (8.854×10^{-14} F/cm) and A is the effective surface area of the electrode. From (12), it is clear that as the thickness of the protective layer, that is, the film formed by inhibitor molecules, increases, the C_{dl} should decrease. In our present studies C_{dl} value was found to be highest for uninhibited solution. Addition of optimum concentration (0.4×10^{-3} M) of inhibitors to the aggressive medium is found to decrease the C_{dl} value and also lowest value is obtained for inhibitor 01 with highest inhibition efficiency, because in this case the inhibitor exists as an equilibrium mixture of both boat and chair form and boat form of the inhibitor could adsorb through both CO and NH groups and the parallel orientation of the plain containing the C-2, C-3, C-5, and C-6 atoms of piperidone ring screens the mild steel surface from the attack of the corrosive media. The inhibition efficiency of inhibitors for the corrosion of mild steel in 1 N H_2SO_4 medium is calculated using R_{ct} values as follows:

$$\text{IE}\,(\%) = R_{ct(i)} - R_{ct(0)} \times \frac{100}{R_{ct(i)}}, \quad (13)$$

where $R_{ct(0)}$ and $R_{ct(i)}$ are the charge-transfer resistance values in absence and presence of inhibitor, respectively. The R_{ct} value was found to be the highest for the inhibitor 01 in both acid media, indicating that the system corrodes slower in 01 when compared to others. The order of inhibition efficiency obtained from R_{ct} values is as follows:

$$(01) > (02) > (06) > (03) > (05) > (04).$$

The inhibition efficiencies obtained from R_{ct} are in good agreement with those obtained from potentiodynamic and weight loss measurements.

3.7. FTIR Spectral Studies. The FTIR spectra of 3-methyl-2,6-diphenylpiperidin-4-one (02) as well as the adsorbed film of this inhibitor over mild steel surface were recorded using Shimadzu IR Affinity-1 spectrometer. The FTIR spectra of the inhibitor and the adsorbed film are shown in Figures 13 and 14. All the variously substituted piperidin-4-ones involved in the present investigation have been shown to exist in the chair conformation with alkyl and phenyl groups in equatorial orientations. Infrared spectroscopy has been proved to be a valuable tool in the analysis of the stereochemistry of heterocyclic compounds, mainly on the basis of a series of bands in the region 2800–2600 cm^{-1} called Bohlmann bands [65]. These bands have also been used in the assessment of conformational equilibria in decahydroquinolines [66] and piperidin systems [67, 68]. Piperidin-4-ones also exhibit these bands in the region 3000–2800 cm^{-1} (Figure 13) and these bands disappear on adsorption through nitrogen (Figure 14) due to the lack of antiperiplanarity with respect to the lone pair of electrons as a result of change in conformation [69]. The sharp peak around 3296 cm^{-1} due to N–H

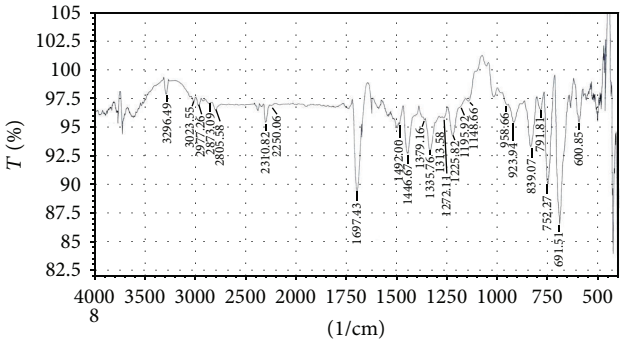

8

Figure 13: FTIR spectrum of t(3)-methyl-r(2),c(6)-diphenylpiperidin-4-one (02).

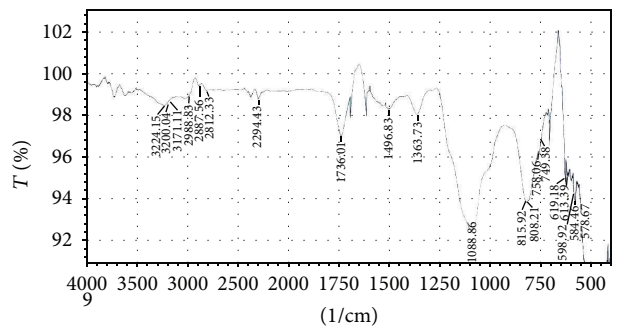

9

Figure 14: FTIR spectrum of corrosion product from mild steel surface after immersion in 1 N H_2SO_4 containing t(3)-methyl-r(2), c(6)-diphenylpiperidin-4-one (02).

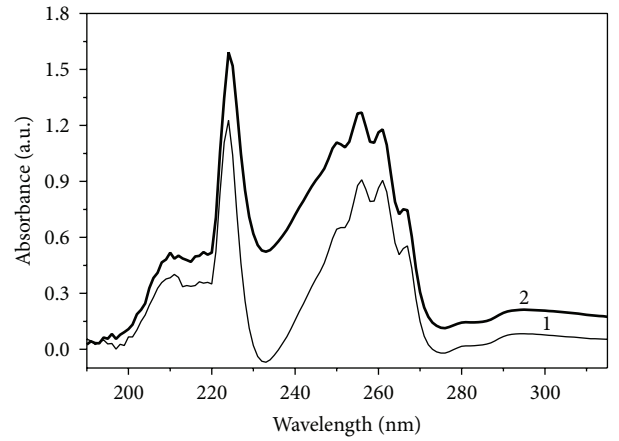

Figure 15: UV spectra of (2×10^{-3} M) t(3)-methyl-r(2),c(6)-diphenylpiperidin-4-one (02) used as inhibitors for mild steel corrosion in 1 N H_2SO_4 solutions [1] before and [2] after weight loss measurements.

stretching of the piperidin-4-one (02) has also been shifted to lower frequency region (3224 to 3171 cm^{-1}) and is broadened in the IR spectrum of the adsorbed film.

The carbonyl stretching frequency of the inhibitor (02) appears at 1697 cm^{-1}. This absorption peak is shifted to higher frequency (1736 cm^{-1}) in the spectrum of adsorbed film.

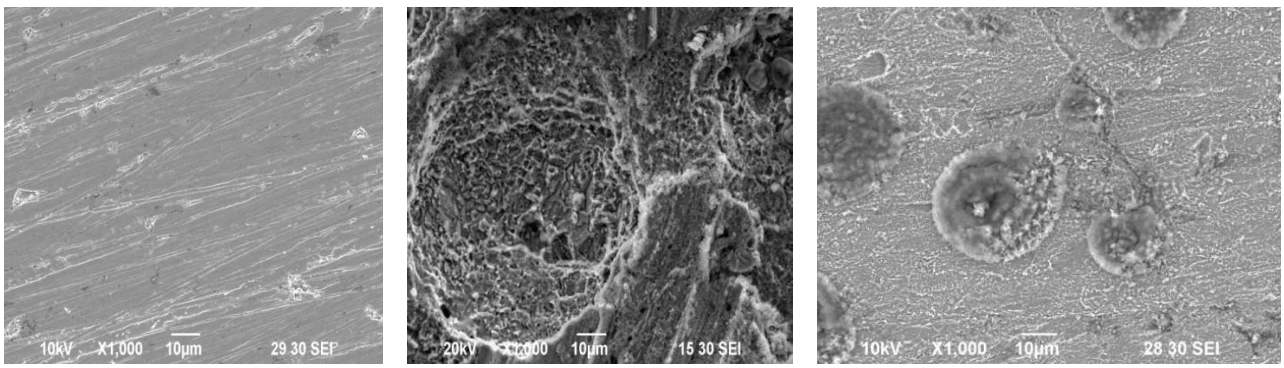

(a) (b) (c)

Figure 16: SEM photographs of mild steel sample (a) polished surface, (b) after immersion in 1 N H_2SO_4 solution, and (c) in the presence of (2×10^{-3} M) inhibitor (02).

Generally ring carbonyl absorption frequency will be shifted to higher frequency as the ring becomes more and more strained [70]; similar high frequency shifts of carbonyl absorption are noted in the piperidin-4-one complexes of cobalt (II), nickel (II), and copper (II) [66].

According to Rengamani et al. [1] the high frequency shift is not attributed to carbonyl participation but due to conformational change of the ring during complex formation through ring nitrogen. The IR spectrum of the free inhibitor (02) shows no appreciable change in the carbonyl shifts due to electron releasing groups. Hence in the present studies it is reasonable to assume that the high frequency shift of carbonyl group in the adsorbed film may be due to the ring strain caused by the interaction between ring nitrogen and mild steel surface. A new band is observed in the spectrum of the adsorbed film in the region 520–508 cm^{-1} and this may be attributed to metal nitrogen bonding.

3.8. UV Absorption Spectra. The UV regions of the electronic spectra of the inhibited solutions before and after immersion of mild steel specimens were recorded using *Shimadzu UV*-1800 spectrometer and are given in Figure 15. The spectra of the inhibited solution before immersion of the mild steel specimens show two bands, a high intensity band at 224 nm and a low intensity band at 256 nm. The low intensity band may be assigned to $n \rightarrow \pi^*$ transition of carbonyl group present in the inhibitors. The high intensity band may be due to $\pi \rightarrow \pi^*$ transition of the carbonyl group as well as phenyl groups. The spectra of the inhibited solution after immersion of mild steel plate show very slight shifts compared with the spectra of inhibited solution before immersion. But the absorption intensity corresponding to the above mentioned bands is high in the inhibited solution after mild steel immersion. This may be attributed to the change in the orientation of the phenyl groups of piperidin-4-ones due to adsorption on mild steel surface. The change in orientation of the phenyl groups leads to increase in ring strain and this is supported by FTIR spectrum of the inhibitor. The substitutional effect studied in this chapter also supports the presence of ring strain.

3.9. Scanning Electron Microscopy (SEM). The discussion presented above makes it clear that piperidin-4-ones are proved to be good inhibitors for mild steel in 1 N H_2SO_4. To confirm the obtained results, electron microscope photographs of mild steel specimen were taken before and after immersion in 1 N H_2SO_4 solution and in the presence of 2.0×10^{-3} M concentration of inhibitor *t*(3)-methyl-*r*(2), *c*(6)-diphenylpiperidin-4-one (02). The SEM photographs are shown in Figures 16(a)–16(c).

Figure 16(a) illustrates the brightly polished surface of the mild steel specimen before immersion in the test solution, while Figure 16(b) depicts the effect of 1 N H_2SO_4 solutions on the mild steel specimen after 1-hour immersion. It clearly shows large pits that are caused by the attack of 1 N H_2SO_4 solution. On comparing these microphotographs with those in Figure 16(c) it is evident that, in the presence of 2.0×10^{-3} M of inhibitor (02), the surface morphology of the mild steel specimen has been changed due to the presence of the adsorbed layer of inhibitor molecules, and the large pits shown in Figure 16(b) in the absence of inhibitor have been reduced and the depth of pits has decreased. Thus the addition of inhibitor (02) to the aggressive medium has reduced the corrosion of mild steel specimen in 1 N H_2SO_4 solution.

4. Conclusion

(1) The various substituted 2,6-diphenyl-methylpiperidine-4-ones (01–06) exhibit maximum efficiency towards the corrosion inhibition of mild steel in 1 N H_2SO_4. The optimum efficiency of these compounds was achieved even at very low concentration of the inhibitors (0.4×10^{-3} M). Thus piperidin-4-ones act as efficient inhibitors. Also, the order of inhibition efficiency is as follows: 01 > 02 > 06 > 03 > 05 > 04. At higher temperatures, the rate of corrosion is less in inhibiting solutions compared with the uninhibited solutions.

(2) Piperidin-4-ones contain two potential anchoring sites, namely, the carbonyl group and the ring

nitrogen; the results indicate the participation of only ring nitrogen.

(3) The increase in apparent activation energy in the inhibited solution suggests physical adsorption of the inhibitors on the mild steel surface.

(4) Positive values of enthalpy of activation (ΔH°) in the inhibited solution reflect the endothermic nature of mild steel dissolution. Also, the positive values of entropy of activation (ΔS°) suggest that an increase in disordering takes place in metal/solution interface.

(5) The values of ΔG°_{ads} indicate that the adsorption of inhibitors on the mild steel surface may involve complex interactions involving both physical and chemical adsorption. The FT-IR and SEM analysis supports the formation of protective film on the mild steel surface.

(6) The adsorption on piperidine-4-ones on mild steel in 1 N H_2SO_4 obeys Langmuir adsorption isotherm.

(7) The variation of Tafel constants b_a, b_c and E_{corr} values with the increase in concentration of piperidine-4-ones (01–06) suggest that these compounds act as mixed type inhibitors.

Conflict of Interests

The authors declare that there is no conflict of interests regarding the publication of this paper.

References

[1] S. Rengamani, S. Muralidharan, M. Anbu Kulandainathan, and S. Venkatakrishna Iyer, "Inhibiting and accelerating effects of aminophenols on the corrosion and permeation of hydrogen through mild steel in acidic solutions," *Journal of Applied Electrochemistry*, vol. 24, no. 4, pp. 355–360, 1994.

[2] S. S. Abd El-Rehim, M. A. M. Ibrahim, and K. F. Khaled, "4-Aminoantipyrine as an inhibitor of mild steel corrosion in HCl solution," *Journal of Applied Electrochemistry*, vol. 29, no. 5, pp. 593–599, 1999.

[3] M. A. Quraishi and D. Jamal, "Inhibition of mild steel corrosion in the presence of fatty acid triazoles," *Journal of Applied Electrochemistry*, vol. 32, no. 4, pp. 425–430, 2002.

[4] K. C. Emregül, R. Kurtaran, and O. Atakol, "An investigation of chloride-substituted Schiff bases as corrosion inhibitors for steel," *Corrosion Science*, vol. 45, no. 12, pp. 2803–2817, 2003.

[5] K. F. Khaled, K. Babic-Samardzija, and N. Hackerman, "Piperidines as corrosion inhibitors for iron in hydrochloric acid," *Journal of Applied Electrochemistry*, vol. 34, no. 7, pp. 697–704, 2004.

[6] H.-L. Wang, R.-B. Liu, and J. Xin, "Inhibiting effects of some mercapto-triazole derivatives on the corrosion of mild steel in 1.0 M HCl medium," *Corrosion Science*, vol. 46, no. 10, pp. 2455–2466, 2004.

[7] F. Bentiss, M. Lebrini, and M. Lagrenée, "Thermodynamic characterization of metal dissolution and inhibitor adsorption processes in mild steel/2,5-bis(n-thienyl)-1,3,4-thiadiazoles/hydrochloric acid system," *Corrosion Science*, vol. 47, no. 12, pp. 2915–2931, 2005.

[8] S. Zor, P. Dogan, and B. Yazici, "Inhibition of acidic corrosion of iron and aluminium by SDBS at different temperatures," *Corrosion Reviews*, vol. 23, no. 2-3, pp. 217–232, 2005.

[9] M. A. Quraishi, D. Jamal, and R. N. Singh, "Inhibition of mild steel corrosion in the presence of fatty acid thiosemicarbazides," *Corrosion*, vol. 58, no. 3, pp. 201–207, 2002.

[10] A. Popova, M. Christov, S. Raicheva, and E. Sokolova, "Adsorption and inhibitive properties of benzimidazole derivatives in acid mild steel corrosion," *Corrosion Science*, vol. 46, no. 6, pp. 1333–1350, 2004.

[11] A. Y. Musa, A. A. H. Kadhum, A. B. Mohamad, M. S. Takriff, A. R. Daud, and S. K. Kamarudin, "Adsorption isotherm mechanism of amino organic compounds as mild steel corrosion inhibitors by electrochemical measurement method," *Journal of Central South University of Technology*, vol. 17, no. 1, pp. 34–39, 2010.

[12] S. Vishwanatham and M. A. Kumar, "Corrosion inhibition of mild steel in binary acid mixture," *Corrosion Reviews*, vol. 23, no. 2-3, pp. 181–194, 2005.

[13] M. B. Balasubramanian and N. Padma, "Studies on conformation-I. Preparation and stereochemistry of some 4-piperidinols," *Tetrahedron*, vol. 19, no. 12, pp. 2135–2143, 1963.

[14] C. R. Noller and V. Baliah, "The preparation of some piperidine derivatives by the Mannich reaction," *Journal of the American Chemical Society*, vol. 70, no. 11, pp. 3853–3855, 1948.

[15] B. Vijayan, *[Ph.D. thesis]*, Annamalai University, Chidambaram, India, 1981.

[16] M. B. Balasubramanian and N. Padma, "Studies on conformation—I: preparation and stereochemistry of some 4-piperidinols," *Tetrahedron*, vol. 19, no. 12, pp. 2135–2143, 1963.

[17] T. M. Ikramuddeen, *[Ph.D. thesis]*, Bharathiar University, Coimbatore, India, 1994.

[18] K. Selvaraj, M. Narasimhan, and J. Mallika, "Cobalt(II) nitrate complexes with piperidin-4-ones," *Transition Metal Chemistry*, vol. 26, no. 1-2, pp. 224–227, 2001.

[19] S. Muralidharan, R. Chandrasekar, and S. V. K. Iyer, "Effect of piperidones on hydrogen permeation and corrosion inhibition of mild steel in acidic solutions," *Proceedings of the Indian Academy of Sciences: Chemical Sciences*, vol. 112, no. 2, pp. 127–136, 2000.

[20] A. N. Senthilkumar, K. Tharini, and M. G. Sethuraman, "Studies on a few substituted piperidin-4-one oximes as corrosion inhibitor for mild steel in HCL," *Journal of Materials Engineering and Performance*, vol. 20, no. 6, pp. 969–977, 2011.

[21] S. Sankarapapavinasam, F. Pushpanaden, and M. F. Ahmed, "Piperidine, piperidones and tetrahydrothiopyrones as inhibitors for the corrosion of copper in H_2SO_4," *Corrosion Science*, vol. 32, no. 2, pp. 193–203, 1991.

[22] A. N. Senthilkumar, K. Tharini, and M. G. Sethuraman, "Corrosion inhibitory effect of few piperidin-4-one oximes on mild steel in hydrochloric acid medium," *Surface Review and Letters*, vol. 16, no. 1, pp. 141–147, 2009.

[23] R. T. Vashi, H. M. Bhajiwala, and S. A. Desai, "Hexamine as corrosion inhibitor for zinc in (HNO_3 + H_2SO_4) binary acid mixture," *Der Pharma Chemica*, vol. 5, no. 2, pp. 237–243, 2013.

[24] K. F. Khaled, K. B. Samardzija, and N. Hackerman, "Piperidines as corrosion inhibitors for iron in hydrochloric acid," *Journal of Applied Electrochemistry*, vol. 34, no. 7, pp. 697–704, 2004.

[25] K. Babić-Samardžija, K. F. Khaled, and N. Hackerman, "*N*-heterocyclic amines and derivatives as corrosion inhibitors for iron in perchloric acid," *Anti-Corrosion Methods and Materials*, vol. 52, no. 1, pp. 11–21, 2005.

[26] S. K. Shukla and E. E. Ebenso, "Corrosion inhibition, adsorption behavior and thermodynamic properties of streptomycin on mild steel in hydrochloric acid medium," *International Journal of Electrochemical Science*, vol. 6, no. 8, pp. 3277–3291, 2011.

[27] I. Ahamad, R. Prasad, and M. A. Quraishi, "Thermodynamic, electrochemical and quantum chemical investigation of some Schiff bases as corrosion inhibitors for mild steel in hydrochloric acid solutions," *Corrosion Science*, vol. 52, no. 3, pp. 933–942, 2010.

[28] I. B. Obot, N. O. Obi-Egbedi, and S. A. Umoren, "Adsorption characteristics and corrosion inhibitive properties of clotrimazole for aluminium corrosion in hydrochloric acid," *International Journal of Electrochemical Science*, vol. 4, no. 6, pp. 863–877, 2009.

[29] A. Zarrouk, B. Hammouti, H. Zarrok, S. S. Al-Deyab, and M. Messali, "Temperature effect, activation energies and thermodynamic adsorption studies of L-Cysteine Methyl Ester Hydrochloride as copper corrosion inhibitor in nitric acid 2M," *International Journal of Electrochemical Science*, vol. 6, no. 12, pp. 6261–6274, 2011.

[30] C. S. Venkatachalam, S. R. Rajagopalan, and M. V. C. Sastry, "Mechanism of inhibition of electrode reactions at high surface coverages—II," *Electrochimica Acta*, vol. 26, no. 9, pp. 1219–1224, 1981.

[31] A. A. Khadom, A. S. Yaro, A. S. Altaie, and A. A. H. Kadum, "Electrochemical, activations and adsorption studies for the corrosion inhibition of low carbon steel in acidic media," *Portugaliae Electrochimica Acta*, vol. 27, no. 6, pp. 699–712, 2009.

[32] E. A. Noor, "Temperature effects on the corrosion inhibition of mild steel in acidic solutions by aqueous extract of fenugreek leaves," *International Journal of Electrochemical Science*, vol. 2, pp. 996–1017, 2007.

[33] M. Lebrini, F. Robert, and C. Roos, "Inhibition effect of alkaloids extract from *Annona squamosa* plant on the corrosion of C38 steel in normal hydrochloric acid medium," *International Journal of Electrochemical Science*, vol. 5, no. 11, pp. 1698–1712, 2010.

[34] I. B. Obot, S. A. Umoren, and N. O. Obi-Egbedi, "Corrosion inhibition and adsorption behaviour for aluminuim by extract of *Aningeria robusta* in HCl solution: synergistic effect of iodide ions," *Journal of Materials and Environmental Science*, vol. 2, no. 1, pp. 60–71, 2011.

[35] I. M. Mejeha, A. A. Uroh, K. B. Okeoma, and G. A. Alozie, "The inhibitive effect of *Solanum melongena* L. leaf extract on the corrosion of aluminium in tetraoxosulphate (VI) acid," *African Journal of Pure and Applied Chemistry*, vol. 4, pp. 158–165, 2010.

[36] D. Ben Hmamou, R. Salghi, A. Zarrouk et al., "Alizarin red: an efficient inhibitor of C38 steel corrosion in hydrochloric acid," *International Journal of Electrochemical Science*, vol. 7, no. 6, pp. 5716–5733, 2012.

[37] M. A. Migahed, H. M. Mohamed, and A. M. Al-Sabagh, "Corrosion inhibition of H-11 type carbon steel in 1 M hydrochloric acid solution by *N*-propyl amino lauryl amide and its ethoxylated derivatives," *Materials Chemistry and Physics*, vol. 80, no. 1, pp. 169–175, 2003.

[38] E. E. Oguzie, B. N. Okolue, E. E. Ebenso, G. N. Onuoha, and A. I. Onuchukwu, "Evaluation of the inhibitory effect of methylene blue dye on the corrosion of aluminium in hydrochloric acid," *Materials Chemistry and Physics*, vol. 87, no. 2-3, pp. 394–401, 2004.

[39] E. E. Ebenso, N. O. Eddy, and A. O. Odiongeny, "Corrosion inhibition and adsorption properties of methocarbamol on mild steel in acidic medium," *Portugaliae Electrochimica Acta*, vol. 27, no. 1, pp. 13–22, 2009.

[40] R. F. V. Villamil, P. Corio, J. C. Rubim, and S. M. L. Agostinho, "Sodium dodecylsulfate-benzotriazole synergistic effect as an inhibitor of processes on copper — chloridric acid interfaces," *Journal of Electroanalytical Chemistry*, vol. 535, no. 1-2, pp. 75–83, 2002.

[41] E. E. Oguzie, Y. Li, and F. H. Wang, "Corrosion inhibition and adsorption behavior of methionine on mild steel in sulfuric acid and synergistic effect of iodide ion," *Journal of Colloid and Interface Science*, vol. 310, no. 1, pp. 90–98, 2007.

[42] I. B. Obot and N. O. Obi-Egbedi, "Ipomoea involcrata as an ecofriendly inhibitor for aluminium in alkaline medium," *Portugaliae Electrochimica Acta*, vol. 27, no. 4, pp. 517–524, 2009.

[43] T. Umasankareswari and T. Jeyaraj, "Salicylideneaniline as inhibitor for the corrosion of mild steel in 1.0 N hydrochloric acid," *Journal of Chemical and Pharmaceutical Research*, vol. 4, no. 7, pp. 3414–3419, 2012.

[44] A. K. Singh and M. A. Quraishi, "Investigation of the effect of disulfiram on corrosion of mild steel in hydrochloric acid solution," *Corrosion Science*, vol. 53, no. 4, pp. 1288–1297, 2011.

[45] M. Bouklah, B. Hammouti, M. Lagrenée, and F. Bentiss, "Thermodynamic properties of 2,5-bis(4-methoxyphenyl)-1,3,4-oxadiazole as a corrosion inhibitor for mild steel in normal sulfuric acid medium," *Corrosion Science*, vol. 48, no. 9, pp. 2831–2842, 2006.

[46] E. E. Ebenso, I. B. Obot, and L. C. Murulana, "Quinoline and its derivatives as effective corrosion inhibitors for mild steel in acidic medium," *International Journal of Electrochemical Science*, vol. 5, no. 11, pp. 1574–1586, 2010.

[47] M. A. Amin, K. F. Khaled, and S. A. Fadl-Allah, "Testing validity of the tafel extrapolation method for monitoring corrosion of cold rolled steel in HCl solutions—experimental and theoretical studies," *Corrosion Science*, vol. 52, no. 1, pp. 140–151, 2010.

[48] A. Łukomska and J. Sobkowski, "Potential of zero charge of monocrystalline copper electrodes in perchlorate solutions," *Journal of Electroanalytical Chemistry*, vol. 567, no. 1, pp. 95–102, 2004.

[49] H. H. Hassan, E. Abdelghani, and M. A. Amin, "Inhibition of mild steel corrosion in hydrochloric acid solution by triazole derivatives. Part I. Polarization and EIS studies," *Electrochimica Acta*, vol. 52, no. 22, pp. 6359–6366, 2007.

[50] M. A. Amin, S. S. Abd El-Rehim, E. E. F. El-Sherbini, and R. S. Bayoumi, "The inhibition of low carbon steel corrosion in hydrochloric acid solutions by succinic acid. Part I. Weight loss, polarization, EIS, PZC, EDX and SEM studies," *Electrochimica Acta*, vol. 52, no. 11, pp. 3588–3600, 2007.

[51] E. E. Ebenso, H. Alemu, S. A. Umoren, and I. B. Obot, "Inhibition of mild steel corrosion in sulphuric acid using alizarin yellow GG dye and synergistic iodide additive," *International Journal of Electrochemical Science*, vol. 3, no. 12, pp. 1325–1339, 2008.

[52] L. Niu, H. Zhang, F. Wei, S. Wu, X. Cao, and P. Liu, "Corrosion inhibition of iron in acidic solutions by alkyl quaternary ammonium halides: correlation between inhibition efficiency and molecular structure," *Applied Surface Science*, vol. 252, no. 5, pp. 1634–1642, 2005.

[53] S. A. Umoren and E. E. Ebenso, "The synergistic effect of polyacrylamide and iodide ions on the corrosion inhibition of mild steel in H_2SO_4," *Materials Chemistry and Physics*, vol. 106, no. 2-3, pp. 387–393, 2007.

[54] Y. Feng, K. S. Siow, W. K. Teo, and A. K. Hsich, "The synergistic effects of propargyl alcohol and potassium iodide on the inhibition of mild steel in 0.5 M sulfuric acid solution," *Corrosion Science*, vol. 41, no. 5, pp. 829–852, 1999.

[55] K. Parameswari, *[Ph.D. thesis]*, Bharathiar University, Coimbatore, India, 2006.

[56] S. A. Umoren, M. M. Solomon, I. I. Udosoro, and A. P. Udoh, "Synergistic and antagonistic effects between halide ions and carboxymethyl cellulose for the corrosion inhibition of mild steel in sulphuric acid solution," *Cellulose*, vol. 17, no. 3, pp. 635–648, 2010.

[57] N. Hackerman and A. C. Makrides, "Inhibition of acid dissolution of metals .1. Some general observations," *Journal of Physics and Chemistry*, vol. 56, p. 707, 1955.

[58] K. Aramaki, M. Hagiwara, and H. Nishihara, "The synergistic effect of anions and the ammonium cation on the inhibition of iron corrosion in acid solution," *Corrosion Science*, vol. 27, no. 5, pp. 487–497, 1987.

[59] B. Sherine, A. J. Abdul Nasser, and S. Rajendran, "Inhibitive action of hydroquinone: Zn^{2+} system in controlling the corrosion of carbon steel in well water," *International Journal of Engineering Science and Technology*, vol. 2, pp. 341–357, 2010.

[60] G. Y. Elewady, A. H. Elaskalany, and A. F. Molouk, "Some β-aminoketone derivatives as corrosion inhibitors for nickel in hydrochloric acid solution," *Portugaliae Electrochimica Acta*, vol. 26, p. 503, 2008.

[61] W. H. Li, Q. He, S. T. Zhang, C. L. Pei, and B. Hou, "Some new triazole derivatives as inhibitors for mild steel corrosion in acidic medium," *Journal of Applied Electrochemistry*, vol. 38, no. 3, pp. 289–295, 2008.

[62] N. Goudarzi, M. Peikari, M. Reza Zahiri, and H. Reza Mousavi, "Adsorption and corrosion inhibition behavior of stainless steel 316 by aliphatic amine compounds in acidic solution," *Archives of Metallurgy and Materials*, vol. 57, no. 3, pp. 845–851, 2012.

[63] S. T. Arab and A. M. Al-Turkustani, "Corrosion inhibition of steel in phosphoric acid by phenacyldimethyl sulfonium bromide and some of its *p*-substituted derivatives," *Portugaliae Electrochimica Acta*, vol. 24, pp. 53–69, 2006.

[64] G. Y. Elewady, "Pyrimidine derivatives as corrosion inhibitors for carbon-steel in 2M hydrochloric acid solution," *International Journal of Electrochemical Science*, vol. 3, no. 10, pp. 1149–1161, 2008.

[65] F. W. Vierhapper and E. L. Eliel, "Conformational analysis. 38. 8-tert-Butyl-trans-decahydroquinolines: carbon-13 and proton nuclear magnetic resonance and infrared spectra. The nitrogen-hydrogen conformational equilibrium," *The Journal of Organic Chemistry*, vol. 44, no. 7, pp. 1081–1087, 1979.

[66] V. Venkatachalam, K. Ramalingam, D. Natrajan, and N. Bhavani, "*bis*(2-Aryldecahydroquinolin-4-onedithiocarbamato)-metal(II) complexes: a new preparative method and characterization along with ^{13}C and ^{1}H NMR decoupling studies," *Synthesis and Reactivity in Inorganic and Metal-Organic Chemistry*, vol. 26, no. 5, pp. 735–759, 1996.

[67] M. Golfier, *Dermination of Configuration by Infrared Spectroscopy*, G. T. Publication, Stuttgart, Germany, 1st edition, 1977.

[68] T. Masamune, M. Tagasugi, and M. Matsuki, "Infrared-spectral studies on the orientation of the lone pairs in piperidine derivatives," *Bulletin of the Chemical Society of Japan*, vol. 41, no. 10, pp. 2466–2472, 1968.

[69] N. Manjula, *[Ph.D. thesis]*, Bharathiar University, Coimbatore, India, 2001.

[70] R. M. Silverstein, G. C. Bassler, and T. C. Morill, *Spectrometric Identification of Organic Compounds*, Wiley, New York, NY, USA, 1978.